Berthelot-type conductivity of porous Sr_2CrReO_6: Examination of an old empirical relation

B. Fisher, K. B. Chashka, L. Patlagan, and G. M. Reisner
Physics Department and Crown Center for Superconductivity, Technion, Haifa 32000, Israel
(Received 17 February 2004; revised manuscript received 20 May 2004; published 8 November 2004)

We report on the linear and nonlinear conductivity of porous samples, and of a cold-pressed powder compact of Sr_2CrReO_6, a ferrimagnetic double-perovskite. The ohmic conductivity (σ) of the porous samples increases exponentially with temperature (it is Berthelot-type) over an unprecedented wide range, from liquid He, up to room temperature. This temperature dependence was predicted by Tredgold for quantum tunneling through a potential barrier of oscillating width. $\sigma(T)$ of the cold-pressed sample follows another famous relation derived by Sheng for his "fluctuation induced tunneling" (FIT) model. This model is applicable to systems consisting of metallic islands separated by insulating barriers. The nonlinear conductivity dependence on electric field and temperature for both types of samples follows the generic behavior of systems with FIT-type ohmic conductivities.

DOI: 10.1103/PhysRevB.70.205109 PACS number(s): 72.20.Ht, 72.25.Mk, 73.40.Gk, 81.05.Rm

I. INTRODUCTION

The empirical Berthelot rate equation,[1] $\ln K = A + BT$ (K—reaction rate, T—temperature, A and B constants) was used in chemistry for many decades since 1862 before being replaced by the Arrhenius rule[2] ($\ln K = C - D/T$) for thermally activated processes. Uncannily, exactly one century later Tredgold[3] predicted $\ln \sigma = A + BT$ for quantum tunneling conductivity (σ) through a potential barrier of oscillating width. In 1985 Hurd[4] elaborated on this model and revealed Berthelot-type $\sigma(T)$ for a number of examples: Indium-doped CdS films, semi-insulating GaAs, As_2Te_3, a disordered AsTeSiGe alloy and Ti_7O_{13}. A more recent example is porous silicon,[5,6] famous for its luminescence[7] (absent in dense silicon). Here we show that the low field conductivity of porous Sr_2CrReO_6[8] (SCRO) exhibits this type of $\sigma(T)$, but over a temperature range much wider than those reported for all the previous examples. On the other hand, the conductivity of a cold-pressed powder compact of this material varies with temperature according to the relation derived by Sheng[9] for his "fluctuation induced tunneling" (FIT) model. In this model, generalized from a single tunnel junction to a random network of junctions, thermally induced voltage fluctuations across vibrating barriers play an important role in determining the temperature and field dependencies of the conductivity. An important prediction of the FIT model[9] is that the degree of $J(E)$ nonlinearity (J—current density) decreases as T increases. This is due to an effective lowering and narrowing of the barrier by voltage fluctuations. This model has been applied successfully to the linear and nonlinear conductivity of many systems consisting of metallic islands separated by insulating barriers, such as carbon composites,[9] heavily doped (disordered) GaAs,[9] conducting polymers,[10,11] carbon nanotubes,[11] K_xC_{70} films,[12] polycrystalline Sm_xC_{60},[13] thin films of doped In_2O_3,[14] and more.

The pioneering work of Hwang *et al.*[15] on spin-polarized inter-grain tunneling in $La_{2/3}Sr_{1/3}MnO_3$ has revealed the important role of grain boundaries in the electronic transport and magnetotransport of ferromagnetic oxides. Half-metallic ferrimagnets with Curie temperatures (T_C) above room temperature (RT) are presently of great interest. Several ordered transition-metal double-perovskites have $T_C > \mathrm{RT}$. The most famous member of this family, Sr_2FeMoO_6 (SFMO) with $T_C \approx 420$ K, has attracted attention due to the large low-field magnetoresistance (MR) exhibited by polycrystalline samples at RT.[16] The resistivity of such samples is much larger than that of the bulk; it is dominated by spin-polarized intergrain tunneling up to RT. A very unusual temperature dependence of the zero-field conductivity of polycrystalline and granular SFMO has recently been reported by us:[17] from liquid He to RT at least, $\sigma(T) = \sigma(0)(1 + T/T_g)$. The values of the two constants, T_g and $\sigma(0)$, are spread over about one, and more than four orders of magnitude, respectively. This remarkably simple behavior of $\sigma(T)$ is very different from that observed in other high-MR systems such as manganites[18] where intergrain conduction could be modeled by a combination of elastic and inelastic tunneling via impurity states. Finding out if a linear $\sigma(T)$ is specific to intergrain tunneling in SFMO only, or could be reproduced in other systems, of the same family at least, was essential.

Sr_2CrReO_6 is the metallic ferrimagnet with the highest T_C (635 K) among the transition-metal ordered double-perovskites.[8] Polycrystalline samples of SCRO prepared by the standard solid-state reaction are porous[8] (dense material is obtained by hot-press sintering). The high T_C and the opportunity to investigate transport and magnetotransport in a porous ferrimagnet have attracted our interest in this system. We found that the porous samples exhibit only modest MR [$\Delta\rho(H)/\rho(0) \approx -0.12$ for $\mu_0 H = 6T$ at low T and drops with increasing T]. However, the importance of the present study stems from the remarkable temperature dependence of the ohmic conductivity (very different from that of polycrystalline SFMO) and the field dependence of the nonohmic conductivity.

II. EXPERIMENT

Porous SCRO samples with densities 40.5% of the ideal were prepared according to the protocol of Ref. 8 (using a compaction pressure of 10 Kbar). X-ray diffraction (XRD)

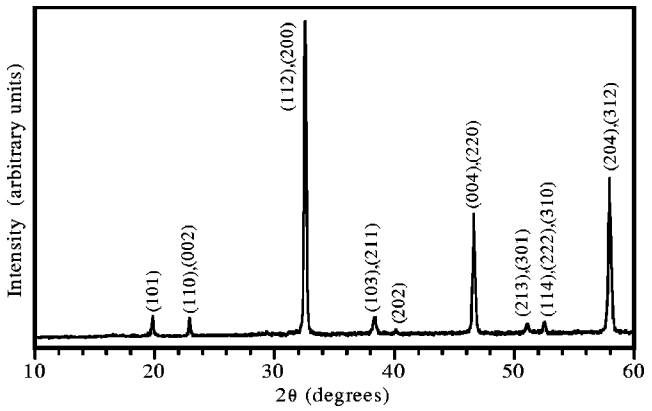

FIG. 1. Indexed XRD powder pattern of Sr_2CrReO_6.

measurements have been performed using a Siemens D5000 powder diffractometer with Cu $K\alpha$ radiation. The XRD powder patterns of the porous SCRO samples showed no foreign phases (see Fig. 1). All the peaks could be indexed in terms of a tetragonal unit cell of space group $I4/mmm$ with $a=5.529(1)$ and $c=7.821(2)$ Å, in good agreement with the results reported in Ref. 8. A porous sample was crushed and cold-pressed into a pellet (using a compaction pressure of 10 Kbar). Its density was 74% of the ideal. The scanning electron microscopy (SEM) micrographs in Fig. 2 were obtained from a porous and a cold-pressed (CP) sample. The estimated averages of the grains' diameters of the porous and CP samples are ~ 1 and ~ 0.4 μm, respectively.

The sintered samples were bar-shaped of lengths $L=1.3$ cm and cross sections A ranging between 0.14×0.28 cm^2 and 0.16×0.29 cm^2. The diameter of the cold-pressed pellet was 0.5 cm and its height was 0.15 cm. The resistivity of the samples was measured by the standard four-probe method in a closed cycle refrigerator or on a cold finger of a He cryostat. The distance between the voltage probes of the bar-shaped samples, l, ranged between 0.50 and 0.59 cm. Four probes were attached also to the circumference of the cold-pressed pellet (in a van der-Pauw configuration). In order to obtain high fields and high current densities for the nonlinear regime of our measurements, thin and short samples are needed (here the entire lengths of the samples are important). A porous sample (S1O) was shortened and thinned by cutting and polishing (L was reduced by a factor of ~ 3, and its new A and l were 0.28×0.044 cm^2 and 0.16 cm, respectively). A bar-shaped sample was cut out from the cold-pressed pellet and was polished. Its final dimensions were $A=0.20\times 0.14$ cm^2, $L=0.4$ cm, and $l=0.13$ cm.

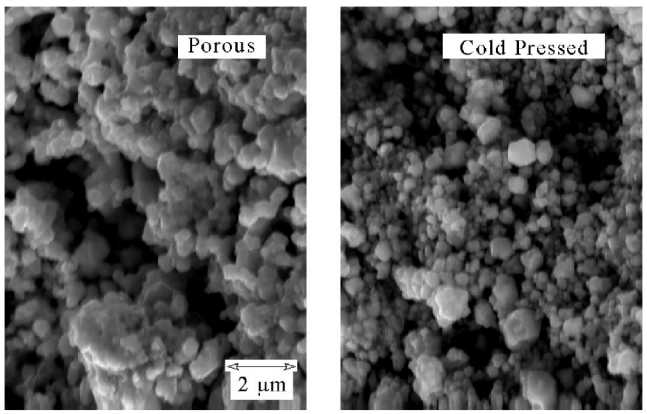

FIG. 2. SEM micrographs of a porous sample and of a cold-pressed powder compact of Sr_2CrReO_6.

In order to prevent Joule heating and verify its absence, high currents were applied using single pulses in the millisecond range from a Keithley 237 high voltage source. The time dependence of the voltage drops between the ground and each of the voltage probes, were recorded using simultaneously the two channels of a Tektronix 2221A digital storage oscilloscope. The current was checked during a second pulse by the voltage drop across a small resistance in series with the sample (it accurately agreed with the nominal current driven from the source). Beyond the finite rise time (in the microsecond range), the measured voltages showed no time dependence during the current pulses. In all the range of our measurements the pulsed current-voltage (I-V) characteristics were reproducible.

III. EXPERIMENTAL RESULTS AND DISCUSSION

Figure 3(a) represents the semilog plots of $\sigma(T)$ for various SCRO samples. The upper two lines are for the fresh S1 and S2 porous samples; S1 was later oxidized in an ambient atmosphere at 400 °C for 15 h (it is labeled S1O). The absolute thermopower S, a property insensitive to grain boundaries was measured on a porous sample. The plot of $S(T)$, shown in the inset, is almost identical to that of the dense material prepared by hot-press sintering,[8] although their resistivities differ by several orders of magnitude. This indicates that the physical properties of the bulk are not affected by microstructure.

The main result of this work is that the three semilog plots of $\sigma(T)$ for the porous samples are almost perfect straight lines, from liquid He temperatures up to RT; they follow the equation

$$\sigma=\sigma(0)e^{T/T_B} \tag{1}$$

with the Berthelot temperature—T_B, ranging from 57 K (for S1) to 77 K (for S2). The effect of oxidation of S1 is mainly on lowering the pre-exponent. The values of T_B for the various examples in Ref. 4 range between 12 and 160 K and for porous silicon,[5,6] between 24 and 100 K. While the validity of Eq. (1) in previous examples is shown over a factor of 4–5 in T (at most), in our results the range is spread over a factor of 20–40. The Tredgold prediction yields[3,4] $k_BT_B\approx\beta a^2/2$, where a is the localization length ($a\propto V^{-1/2}$ with V—the barrier's height) and β, the restoring force constant ($=m\omega^2$, m—the ionic mass and ω—an infrared frequency of an optical phonon). For $a=10^{-10}$ m, $m=10^{-25}$ Kg and $\omega=10^{12}$ s^{-1}, the value of T_B is 73 K. It should be pointed out that Tredgold's model is not the only one leading to Berthelot-type behavior. In more recent models,[19,20] the thermally averaged tunneling probability of a carrier traversing a static barrier may also lead to such behavior. The *exponential* $\sigma(T)$ of porous SCRO is in strong contrast with the *linear* $\sigma(T)$

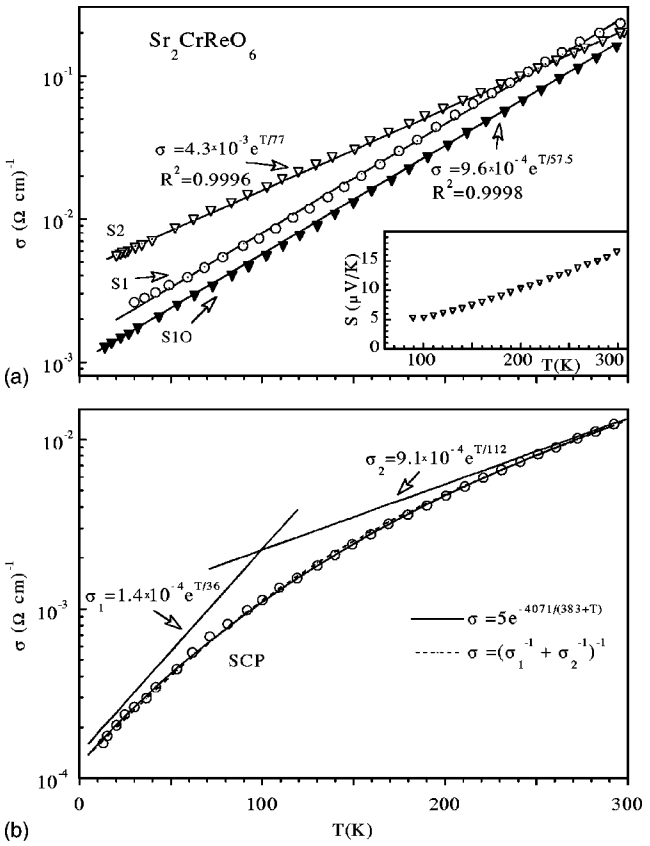

FIG. 3. Temperature dependence of the conductivity of porous samples (S1, S2, and S1O) (a) and of a cold-pressed powder compact (SCP) of Sr_2CrReO_6 (b). Inset: The absolute thermopower of porous Sr_2CrReO_6.

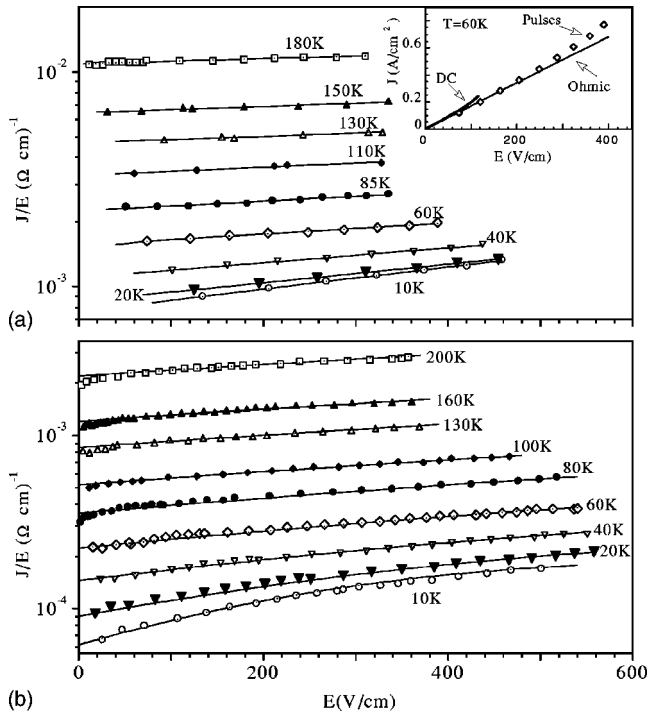

FIG. 4. Nonlinear conductivity represented by isothermal plots of J/E vs E for a porous sample (a) and the powder compact (b). Inset: Comparison of dc and pulsed J-E characteristics emphasizing the effect of Joule heating in dc measurements.

exhibited by sintered and granular SFMO samples.[17] It is possible that this is correlated with the weak MR of the first system as compared to that of the second.

Figure 3(b) represents the semilog plot of $\sigma(T)$ for the CP sample (labeled SCP). The function $[d\ln(\sigma)/dT]^{-1}$ (equivalent to T_B) increases from 35 K at low-T to 112 K at RT, in the ballpark of the values of T_B obtained from the straight lines in Fig. 3(a), indicating that the transport mechanism has not changed much. On the other hand, the solid line fitted to this plot follows the FIT model formula[9]

$$\sigma = \sigma_0 e^{-T_1/(T+T_0)}, \tag{2}$$

where σ_0, T_1, and T_0 are constants; $T_1/T_0 \sim w/a$, where w is the barrier's width and a—the localization length (as earlier); $k_B T_1$ is the activation energy of the process that dominates transport for $T \gg T_0$ (not necessarily hopping above the barrier[9]). The fitted parameters seem reasonable, $T_1/T_0 \approx 10$ and $k_B T_1 \approx 0.35$ eV. It should be mentioned that FIT-type $\sigma(T)$ (with much lower values of T_1 and T_0) has been recently observed for Ag and Na-doped SFMO.[21]

In the course of our search for a possible relation between the Berthelot and FIT-type behaviors, we realized that there may be an alternative interpretation of $\sigma(T)$ for the CP sample. The dashed line in Fig. 3(b), almost indistinguishable from the solid line represents $\sigma(T) = (\sigma_1^{-1} + \sigma_2^{-1})^{-1}$ where $\sigma_1(T)$ and $\sigma_2(T)$ are two Berthelot-type conductivities: $\sigma_2(T)$ is the tangent to the experimental data at RT and $\sigma_1(T)$ is parallel to the tangent to the data at low T, slightly shifted from it by the small value of $\sigma_2^{-1}(0)$. This implies that while the porous samples behave as if their tunnel junctions are of a single type, the CP sample seems to contain a distribution of Berthelot-type junctions; two resistivities with different exponents and preexponents are sufficient to reproduce the experimental data. According to this interpretation, $\sigma(T)$ for this sample is dominated mainly by $\sigma_1(T)$ at very low T and by $\sigma_2(T)$ at high T.

Four-probe I-V characteristics of samples prepared from S1O and SCP were measured between 10 and 200 K using pulsed currents. Thinner and shorter samples enabled the use of high current densities (J) and fields (E). The effect of cold work (see Sec. II) on $\sigma(T)$ was negligible for S1O but serious for the fragile SCP; in the latter case $\sigma(T)$ dropped by a factor of $\sim$2.5 preserving approximately the previous T dependence ($[d\ln(\sigma)/dT]^{-1}$ for the new plot varies from 31 K at low T to 120 K at RT). The nonlinear conductivity results are presented in Fig. 4(a) (for S1O) and (b) (for SCP) as isothermal plots of J/E vs E. J-E characteristics measured with direct current (dc) and with pulsed currents are shown in the inset of Fig. 4(a); this shows that nonohmic behavior due to Joule heating in dc measurements becomes significant at relatively low fields. Thus, the use of pulsed measurements was unavoidable. The solid lines in Fig. 4(a) represent $J/E = \sigma(T)\exp(E/E_0)$. Their extrapolations to $E=0$, are in very good agreement with $\sigma(T)$ measured with very low (dc) currents [see Fig. 5(a), vertical axis at right]. The nonlinear

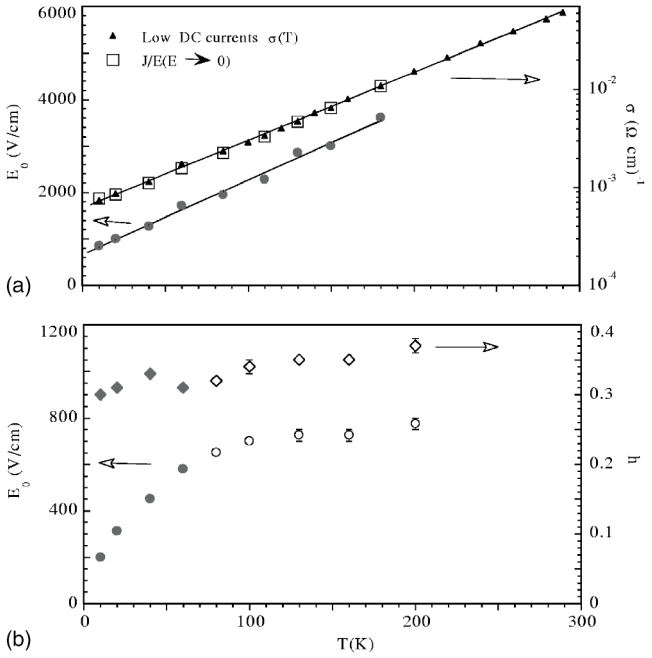

FIG. 5. The temperature dependence of the nonlinear conductivity parameter E_0 for the porous sample (a) and the powder compact (b). $\sigma(T)$ obtained from the extrapolations of the fitted lines in Fig. 4(a) to $E=0$ compared with that measured with low dc currents (a) and the temperature dependence of the second nonlinear conductivity parameter h (b). Bold symbols in (b) represent the fitted parameters of curves with correlation coefficients $R^2 \geqslant 0.99$.

conductivity parameter, E_0 is plotted as function of T in Fig. 5(a) (left vertical axis). In our range of measurements E_0 increases linearly with T. The behavior of J/E vs E of SCP [Fig. 4(b)] is different; over wide ranges of fields the increase of J/E with E is quasilinear (on the semilog scale the plots are curved). The lines fitted to these plots will be discussed later. A theory addressing the nonlinear regime of samples with Berthelot-type $\sigma(T)$ is lacking. An analytic formula for $J(E)$ was derived by Sheng[9] for the FIT model, however, this formula is not valid for too low or too high currents; in the general case numerical calculations are involved in the analyses of experimental results. A generic shape of the *I-V* characteristic was obtained by Kaiser *et al.*[22] on the basis of such calculations. It is well described by the simple analytic expression

$$I = G_0 V \frac{\exp(V/V_0)}{1 + h[\exp(V/V_0) - 1]}. \tag{3}$$

For low fields, this expression reduces to Ohm's law (G_0—the ohmic conductance). Equation (3) expressed in terms of E, E_0, J, and σ, with $h \ll 1$, describes exactly the behavior of the nonlinear conductivity of the porous sample [Fig. 4(a)]: J/E increases exponentially with E on a scale determined by E_0. h is a parameter which damps the exponential increase when tunneling occurs close to the top of the barriers.[22] The field dependence of the denominator becomes significant when E/E_0 approaches $\ln[(1-h)/h]$. This is not observed for the range of fields employed in the measurements on the porous sample. When h is a large fraction of 1, implying shallow barriers, the increase of J/E is slower than exponential over the whole range of fields. The solid lines in Fig. 4(b) represent Eq. (3) with finite h fitted to the experimental data. At low temperatures, the agreement between the calculated lines and the experimental data is very good for the whole range of fields ($R^2 \geqslant 0.99$ for $T=10-60$ K); according to the interpretation based on junctions connected in series, in this range of temperatures transport is dominated by a single type of junctions (represented by σ_1^{-1}). As T increases this agreement becomes gradually poorer ($0.93 \leqslant R^2 \leqslant 0.98$). Above 80 K, in the temperature range around the crossover [see Fig. 3(b)], the fits are valid for not too low fields. The fitting parameters E_0 and h are plotted as function of T in Fig. 5(b) (left and right axes, respectively); the fitted parameters obtained below 60 K are represented by full symbols, the others by empty ones. Although transport in the CP sample is not as straightforward as in the porous sample, the validity of Eq. (3) for the analysis of the low temperature data in Fig. 3(b) seems credible. In this range E_0 increases with T.

It is remarkable that the field dependence of the nonlinear conductivity of samples with Berthelot-type ohmic conductivities, follows the rule discovered for samples with FIT-type ohmic conductivity. This may indicate that the generic shape expressed by Eq. (3) is not too sensitive to the precise nature of the mechanisms involved in transport. It may also indicate that the FIT and Berthelot-type conductivities are related in general, and the relation found in this work is not accidental. It is notable that the increase of E_0 with T for both types of samples is qualitatively consistent with the prediction of the FIT model that the $J(E)$ nonlinearity decreases as T increases.

IV. SUMMARY

To summarize, we have shown that $\sigma(T)$ of porous Sr_2CrReO_6 follows the Berthelot equation, similarly to other systems such as porous silicon, but over a much wider temperature range. Changing the microstructure by grinding and cold pressing leads to $\sigma(T)$ that follows the prediction of the FIT model or alternatively that caused by two Berthelot-type resistivities connected in series. The pulsed, high E-field J-E characteristics of both types of samples follow the same rule and are, at least in qualitative agreement with the prediction of the FIT model. Hopefully, this report will kindle renewed theoretical interest in these models that may ultimately lead to closing the gap between them.

ACKNOWLEDGMENTS

Erudite comments by A. B. Kaiser (Victoria University, N.Z.) and fruitful discussions with A. Mann (Technion) are gratefully acknowledged. The authors are indebted to R. Brenner (Technion) for the SEM micrographs.

[1] M. Berthelot, Ann. Chim. Phys. **66**, 110 (1862). The rate equation does not appear explicitly in this paper but can be derived by plotting the data on p. 116.
[2] For a historical review see: K. J. Laidler, J. Chem. Educ. **61**, 494 (1984).
[3] R. H. Tredgold, Proc. Phys. Soc. London **80**, 807 (1962).
[4] C. M. Hurd, J. Phys. C **18**, 6487 (1985).
[5] J. J. Mareš, J. Krištofik, J. Pangrác, and A. Hospodková, Appl. Phys. Lett. **63**, 180 (1993).
[6] R. M. Mehra, V. Agarwal, V. A. Singh, and P. C. Mathur, J. Appl. Phys. **83**, 2235 (1998).
[7] A. G. Cullis and L. T. Canham, Nature (London) **353**, 335 (1991).
[8] H. Kato, T. Okuda, Y. Okimoto, Y. Tomioka, Y. Tekenoya, A. Ohkubo, M. Kawasaki, and Y. Tokura, Appl. Phys. Lett. **81**, 328 (2002).
[9] P. Sheng, E. K. Sichel, and J. I. Gittleman, Phys. Rev. Lett. **40**, 1197 (1978); P. Sheng, Phys. Rev. B **21**, 2180 (1980).
[10] A. Philipp, W. Mayr, and K. Seeger, Solid State Commun. **43**, 857 (1982).
[11] A. B. Kaiser, Rep. Prog. Phys. **64**, 1 (2001); Adv. Mater. (Weinheim, Ger.) **13**, 927 (2001).
[12] Z. H. Wang, M. S. Dresselhaus, G. Dresselhaus, K. A. Wang, and P. C. Eklund, Phys. Rev. B **49**, 15 890 (1994).
[13] X. H. Chen, S. Y. Li, G. G. Qian, K. Q. Ruan, and L. Z. Cao, Phys. Rev. B **57**, 10 770 (1998).
[14] J. Ederth, P. Johnsson, G. A. Niklasson, A. Hoel, A. Hultåker, P. Heszler, C. G. Granqvist, A. R. van Doorn, M. J. Jongerius, and D. Burgard, Phys. Rev. B **68**, 155410 (2003).
[15] H. Y. Hwang, S.-W. Cheong, N. P. Ong, and B. Batlogg, Phys. Rev. Lett. **77**, 2041 (1996).
[16] K.-I. Kobayashi, T. Kimura, H. Sawada, K. Terakura, and Y. Tokura, Nature (London) **395**, 677 (1998).
[17] B. Fisher, K. B. Chashka, L. Patlagan, and G. M. Reisner, Phys. Rev. B **68**, 134420 (2003).
[18] K. B. Chashka, B. Fisher, J. Genossar, A. Keren, L. Patlagan, G. M. Reisner, E. Shimshoni, and J. F. Mitchell, Phys. Rev. B **65**, 134441 (2002), and references therein.
[19] R. A. Street, Adv. Phys. **25**, 397 (1976).
[20] M. Kapoor, V. A. Singh, and G. K. Johri, Phys. Rev. B **61**, 1941 (2000).
[21] B. Fisher, K. B. Chashka, L. Patlagan, and G. M. Reisner, Curr. Appl. Phys. **4**, 518 (2004).
[22] A. B. Kaiser, S. A. Rogers, and Y. W. Park, Mol. Cryst. Liq. Cryst. **415**, 115 (2004).